

THE DEPOSITION AND CONTROL OF SELF ASSEMBLED SILICON NANO ISLANDS ON CRYSTALLINE SILICON

RAGNAR KIEBACH

*Department of Electronics, INAOE, Apdo. 51,
Puebla, Pue. 72000, Mexico
rkie@inaoep.mx*

ZHENRUI YU*

*Department of Electronics, INAOE,
Puebla, Pue. 72000, Mexico
zyu@inaoep.mx*

MARIANO ACEVES-MIJARES

*Department of Electronics, INAOE,
Puebla, Pue. 72000, Mexico
maceves@inaoep.mx*

DONGCAI BIAN

*College of Materials Science and Chemical Engineering, Tianjin polytechnical University,
Tianjin, China
biandc@tjpu.edu.cn*

JINHUI DU

*College of Materials Science and Chemical Engineering, Tianjin polytechnical University,
Tianjin, China
jinhuilh66@yahoo.com*

The formation of nano sized Si structures during the annealing of silicon rich oxide (SRO) films was investigated. These films were synthesized by low pressure chemical vapor deposition (LPCVD) and used as precursors, a post-deposition thermal annealing leads to the formation of Si nano crystals in the SiO₂ matrix and Si nano islands (Si nI) at c-Si/SRO interface. The influences of the excess Si concentration, the incorporation of N in the SRO precursors, and the presence of a Si concentration gradient on the Si nI formation were studied. Additionally the influence of pre-deposition substrate surface treatments on the island formation was investigated. Therefore, the substrate surface was mechanical scratched, producing high density of net-like scratches on the surface. Scanning electron microscopy (SEM) and high resolution transmission electron microscopy (HRTEM) were used to characterize the synthesized nano islands. Results show that above mentioned parameters have significant influences on the Si nIs. High density nanosized Si islands can epitaxially grow from the c-Si substrate. The reported method is very simple and completely compatible with Si integrated circuit technology.

Keywords: Si nano islands, self assembly, epitaxial growth, silicon-rich oxide, photoluminescence.

* Corresponding author. Tel: +52-222-2663100 ext 8222, Fax: +52-222-247 0517.

1. Introduction

Formation of a regular array of semiconductor nano structures on crystalline Si substrates, especially the formation of silicon islands or dots, is crucial for future applications like single electron devices [1,2], photonic-crystal-based devices [3], single electron memories [4] or quantum dot transistors [5]. Without a doubt, Si nano islands have several advantages over other kinds of nano structured semiconductors. Silicon is the most important electronic material for the ICs industry. Si nano islands grown on c-Si substrates do not have lattice mismatch as in the case of Ge nano islands on Si substrates [6-10], so integration in IC's is significant easier. To observe quantum size effects in Si at room temperature, structures have to be nano sized. Obtaining particles of size of less than 10 nm are a challenge. Even for new approaches like scanning probe microscopy [11,12] or high resolution lithography, which are both complex and time consuming methods and not appropriate for high-throughput methods used in the IC industry. An attractive alternative method is the self-organized formation of Si nIs. To obtain Si nano structures between 1-5 nm range a large variety of techniques has been proposed: ion implantation of Si into SiO₂ [13,14], magnetron sputtering of Si and SiO₂ [15,16], laser ablation of Si targets [17], thermal evaporation of SiO [18,19], Plasma Enhanced Chemical Vapor Deposition (PECVD) and LPCVD.

Recently, we reported that Si nIs on c-Si can be obtained in a simple way by using LPCVD and thermal annealing [20]. Besides that LPCVD is simple and easy for processing, this method is also compatible with common silicon technology and has many advantages over other fabrication methods [21-24]. For future applications it is important to investigate if the formation of Si nIs with this method can be controlled by some processing parameters in order to obtain desired nI sizes and densities. In this report we investigated the influence of several parameters on the formation of Si nIs. The first parameters we studied were the amount of excess silicon and the incorporation of nitrogen. Also the influence of concentration gradients, which were obtained by using a double-layer structure, within the sample was investigated. First a thin layer with high silicon content was deposited, followed by a thick layer with a low silicon excess. This alignment gives the opportunity to investigate the influences of diffusion and oxidation processes on the formation of Si nano structures during the deposition and the thermal annealing. Besides above mentioned structural features also the photoluminescence (PL) of the top layer and the influence of the layer underneath on the PL were examined. Such devices with both controllable Si nIs on the substrate surface and high luminescent layer on the top are interesting for application. The Si nIs in the bottom can be used to fabricate nanoscale electronic devices (such as transistors), while the top layer can be used to prepare optical components. Such nanoscale optical-electronic integration can be achieved by using the proposed structure that has the capability for single photo detection [25]. The last modified synthesis parameter was the substrate surface. The Roughness of the substrate was increased scratching the surface. The formation of Si nIs near the edge and inside the scratches was investigated. The knowledge generated in these experiments allows to influence and control the formation of Si nIs in a remarkable range.

2. Experimental Section

The single SRO layers were deposited on c-Si (100) substrates using LPCVD. Silane (SiH_4) and nitrous oxide (N_2O) were used as the reactive gases, and the partial pressures ratio ($R_o = P_{\text{N}_2\text{O}}/P_{\text{SiH}_4}$) was varied from 10 to 30. SRO doped with nitrogen (represented by SRO:N) was prepared by adding 10% of NH_3 ($P_{\text{NH}_3}/(P_{\text{SiH}_4}+P_{\text{N}_2\text{O}}) = 10\%$) during the deposition. The substrate temperature was 700°C . The deposited SRO layers contain an average excess Si concentration of 13% to 4% as R_o increases from 10 to 30 [26]. For some samples, the c-Si substrate was scratched before the deposition. The scratches are $\sim 10\ \mu\text{m}$ width and 60 to $300\ \mu\text{m}$ separated. The thickness (t_{ox}) of the single SRO films is $\sim 580\ \text{nm}$. For the double-layer sample ($R_o = 5/20$), a thin SRO layer with $R_o = 5$ was first deposited, followed by the deposition of the second SRO layer with $R_o = 20$. For the $R_o = 5/20$ multi-layer samples the thicknesses of the double layers are 40 and 500 nm, respectively. Each deposited sample was divided into two parts and one part was thermally annealed in a N_2 ambient at 1100°C for 3 hours. Table 1 lists the studied samples and their preparation parameters.

Table 1: Nomenclature and some characteristics of samples used.

Sample	R_o ($P_{\text{N}_2\text{O}}/P_{\text{SiH}_4}$)	NH_3 (%)	Thickness (nm)	Annealing ($1100^\circ\text{C}/3\text{hrs}$)	Substrate scratched
SRO10	10	0	580	Yes	No
SRO15	15	0	580	Yes	No
SRO20	20	0	580	Yes	No
SRO30	30	0	580	Yes	No
SRO:N	10	10	580	Yes	No
SRO10SCR	10	0	250	Yes	Yes
SRO5/20	5/20	0	40/500	Yes	No

Scanning electron microscopy (SEM, FEI Quanta 200, 25 kV) and high resolution transmission electron microscopic (HRTEM, Tencai F30 operated with an acceleration voltage of 300 kV, line resolution of 0.2 nm) were used to characterize the structure of the samples.

PL at room temperature was carried out with a Perkin Elmer luminescence spectrometer model LS50B, which is controlled by computer. The samples were excited using a 250 nm (4.96 eV) radiation. PL measurements were scanned between 400 and 900 nm (3.1–1.37 eV) with a resolution of 2.5 nm.

3. Results and Discussion

3.1. Influence of the silicon content

Planar view TEM measurements were performed in order to study the microstructure of the Si nano crystals formed in the SiO₂ matrix. Fig. 1 shows the micrographs of the annealed SRO films with Ro = 10, 15, 20 and 30, respectively.

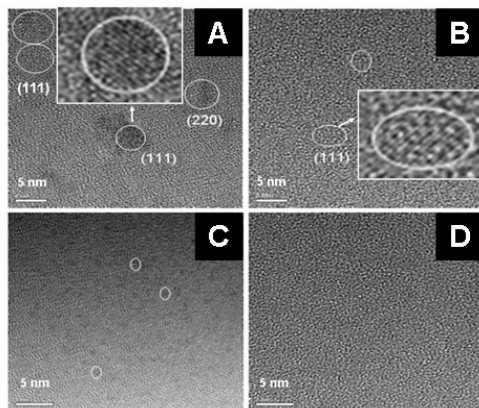


Fig. 1. Planar view TEM micrographs of annealed SRO films deposited with Ro=10 (A), 15 (B), C (20), and D (30), respectively. The scale bars are 5 nm in all the four micrographs. The inset in (A) and (B) shows a single Si nanocrystal of (111) orientation, respectively.

Si nano crystals can be clearly observed in SRO with Ro = 10 and 15 (A and B), which show different orientations as indicated in the figure. The insets in Fig. 1(A) and 1(B) show Si nano crystals with (111) orientation for clarity. For Ro = 20 some amorphous Si nano clusters (black dots in the TEM picture) were found, but these clusters are very small (<1 nm) and no crystalline structure was observed. In samples with Ro = 30 the amorphous Si clusters cannot be detected at all. This indicates that Si nano crystals cannot be formed in SRO with low excess Si concentration (<6%).

Fig. 2 shows cross-section TEM images of an annealed sample (Ro = 10). From Fig. 2(A) of the lower resolution image, one can see that Si nIs are formed at the c-Si/SRO interface with a density of $\sim 7 \times 10^{11} / \text{cm}^2$. The lateral size of the nano islands is 10-20 nm and their height is 4-9 nm. The Si nIs can be free of defects as shown in Fig. 2(D), or have some defects such as dislocations (Fig. 2(B) and 2(C)). In all cases the Si nIs have a crystalline structure. The Si nIs can epitaxially grow from the substrate (Fig. 2 (D)). In some cases (Figs. 2(B) and 2(C)) a thin amorphous intermediate layer is observed between the substrate and the Si nIs. The intermediate layer could be due to be oxygen incorporation, and careful substrate cleaning or treatment (e.g. HF etching) before loaded into the deposition chamber could prohibit this thin intermediate layer and thus epitaxial growth of all the Si nIs is expected to occur. However, even with the intermediate layer, the Si nIs have the same crystalline orientation as the c-Si substrate, as shown in Fig. 2(B,

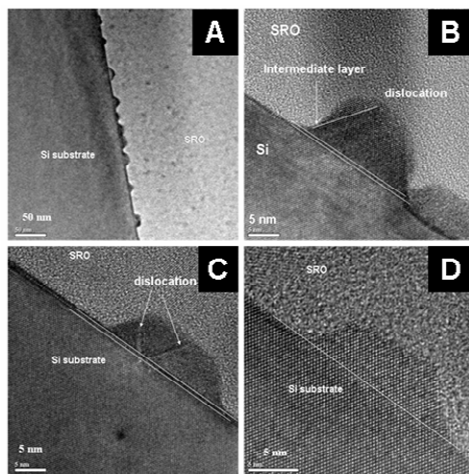


Fig. 2. Cross-section TEM images of SRO films on c-Si after thermal annealing, where (A) was taken with lower resolution, while (B), (C) and (D) were with higher resolution.

and C). The formation of Si nIs on c-Si could be explained by a model of high temperature diffusion and solid-phase crystallization of excess Si in the SRO layers [20]. The formation of Si nIs is very sensitive to the amount of excess Si in the SRO precursors. We investigated the influence of excess Si concentration on the size and density of Si nIs. If the excess Si concentration is high ($\sim 13\%$ Si_{ex}) Si nIs were very easily formed on the c-Si substrate. Sometimes, large Si zones can be formed although some defects such as dislocation are involved. On the other hand, if the excess Si concentration is lower than 8% in SRO films (e.g. SRO with $R_o = 20$ and 30) no Si nIs were formed on the substrate surface. The formation of the Si nIs requires a threshold value of the excess Si concentration in SRO films and a value of $\sim 8.7\%$ (corresponding to $R_o = 15$,) is the lowest limit for the nano islands formation. In this case, a lower density and smaller sizes of Si nIs were observed compared to the $R_o = 10$ samples, as shown in Fig. 3. From Fig. 3(A and B), the nano islands density of $\sim 3 \times 10^9 / \text{cm}^2$ and vertical size of ~ 5 nm was estimated. Also, there are no defects, such as dislocation, inside a Si nIs, and overlapping of adjacent nano islands were not observed. This is in contrast to $R_o = 10$ where either overlapping (as shown in Fig. 2(B)) or dislocation (as shown in Fig. 2(C)) are observed. This result clearly indicates that excess Si concentration in SRO is a key factor for the formation of Si nIs on c-Si substrate, and the ratio R_o is a good process parameter for controlling the Si nI formation.

3.2. Influence of the Nitrogen Incorporation

We also observed that the formation of Si nIs depends on the N incorporation into the SRO. Adding 10% of NH_3 to the reactive gases, the formation of Si nIs was modified. Cross-section TEM images of a SRO:N sample prepared using $R_o = 10$ with 10% of NH_3 addition are shown in Fig.3 (C and D). One can find that the size and density of the Si nIs

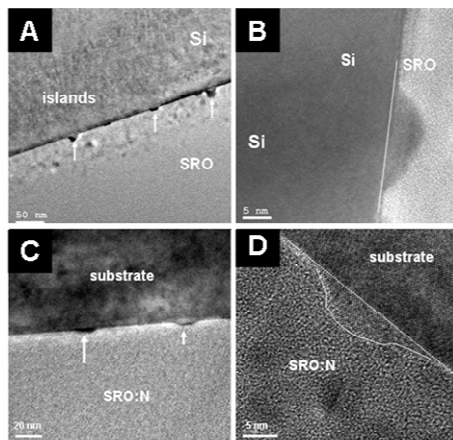


Fig. 3. Cross-section TEM images of SRO and SRO:N films on c-Si after thermally annealing, where A and B are for SRO with $Ro=15$, C and D are for SRO:N.

decrease compared to the SRO of same $Ro = 10$. The estimated density and vertical size of the Si nIs in SRO:N are $\sim 1.6 \times 10^{10} / \text{cm}^2$ and $\sim 3\text{-}5$ nm, respectively. Thus smaller nano islands sizes are obtained. However, if compared with SRO of $Ro = 15$, this SRO:N sample showed higher Si nIs density. Thus, N can reduce the island size while keeping relatively higher island density. Two factors are responsible for the change in size and density of the nano crystals. On one side, the N atoms and clusters may serve as nucleation sites on the starting of the deposition or thermal annealing processes, thus increasing the Si nIs density (compared with SRO15). On the other side, N hinder the diffusion of Si atoms and prevents the phase separation in the amorphous SRO:N films [27]. Thus the mobility of the Si atoms is smaller and the growth of the Si nIs during the thermal diffusion process is reduced, producing smaller islands.

3.3. Multi-Layer Approach

In the cross-section TEM images of $Ro = 5/20$ the two layers are clearly observable (Fig. 4(A) and 4(B)). In Fig. 4(C) one can see that Si nIs at the c-Si/SRO interface are formed. Also, Si nano crystals in the SiO_2 matrix in the $Ro = 5$ layer are observable (Fig. 4(D)). In the much thicker $Ro = 20$ layer no Si nano structures were found (Fig. 4(B) and (C)), coincident with results mentioned above. These results show that it is possible to obtain Si nIs by using a thin Si rich layer. This layer provides the necessary crystal seeds for the first building steps and the necessary amount of excess Si for the further growing of the Si nIs. Compared with $Ro = 10$ the Si nIs in this sample are distributed more irregular (Fig. 4(C) and the density is lower. Also, the shape of the islands is less uniform; the differences in lateral size and height are significant higher. Defects like dislocation or an amorphous intermediate layer as described for $Ro = 10$ were not found. It is surprising that lower nIs density was obtained in the bottom SRO5 layer compared to the SRO10 single layer. One possible reason is due to the very small thickness of the SRO5 layer.

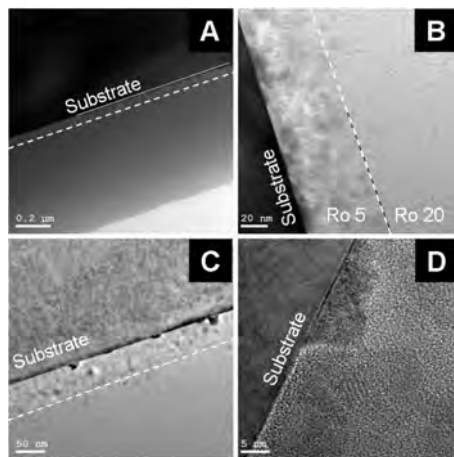


Fig. 4. Cross-section TEM images of SRO5/20 films on c-Si after thermal annealing, where A and B were taken with lower resolution, while C and D were with higher resolution. The dotted lines in A, B and C indicate the interfaces between two SRO layers. The solid line in A indicates the c-Si/SRO interface.

The sharp boundary line between the two different layers indicates that diffusion and oxidations processes are almost negligible. It seems to be unlikely that, during the deposition of the second layer, significant amounts of the reactant gases diffuse into the $Ro = 5$ layer (a phenomena well known in the oxidation of Si). Also during the annealing at $1100\text{ }^{\circ}\text{C}$, the diffusion of Si from the Si-rich layer to the Si-poor layer plays no role, Si nano structures are only found in the $Ro = 5$ layer.

While for the formation of Si nIs high amounts of excess Si are necessary (an excess Si concentration of $\sim 8.7\%$ is the lowest limit), on the contrary, the photoluminescence of SRO requires low silicon excess. In the last years many articles describing the optical properties of SRO materials were published [26,28-29]. The highest PL intensities are found for samples with a low Si content ($Ro = 20$ or $Ro 30$), in which the emission centers could be excess Si related defects [26]. The here used multi-layer approach gives

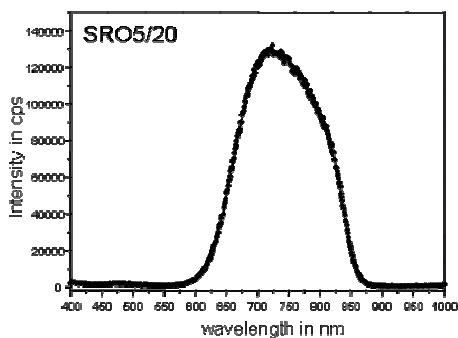


Fig. 5. PL for SRO5/20 double layer in the region from 400 nm to 1000 nm.

the opportunity to investigate the influence of adjacent layers with a different amount of excess Si. In Fig. 5 the PL of for $R_o = 5/20$ is shown. A high intensity in the red region (~ 720 nm) is observed. This result is comparable with results published for $R_o = 20$ single layers, showing that the thin $R_o = 5$ layer has no negative influence on the emissive properties of the top layer, neither the poorer layer influences the characteristic of the under layer. On the other hand, the results demonstrate that is possible to combine the interesting optical and structural properties of single SRO layers using the multi-layer approach, a step towards the integration of optical and electronic data processing circuits on the same chip.

3.4. Influence of substrate surface roughness

Fig.6 shows the effect of substrate surface scratching on the formation of Si nIs. Typical SEM micrographs of the surface of the SRO layer are shown in Fig. 6(A) and 6(B). The growth of the SRO is quite different at the smooth zone and at the scratches region: the growing particles are larger at the scratched region than that at the smooth zone. Also, the particles are regularly arranged along the scratches, with smaller particles formed for shallow scratches (Fig.6B). That indicates that the scratches modify the growth of the SRO layer, and the relatively larger particles with uniform sizes preferably grow at the edges of the scratches. Fig.6(C) and 6(D) show a cross-section TEM graphs near the edge of the scratches. It is found that pyramid-like Si islands can be formed at the edge of the scratches. Then, the scratches can affect the formation of Si nIs and probably determine the location and shape of the Si nIs on c-Si substrate. In order to have a better control of the Si nIs formation, the scratches should be as sharp as possible. Chemical etching of the Si substrates with desired patterns could be a better choice than the mechanic scratching that cannot produce sharp scratches with complex patterns.

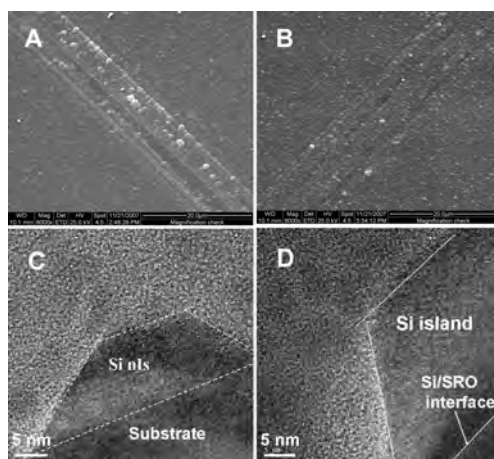


Fig. 6. Surface morphology (A and B) and cross section TEM micrographs of the SRO layer near the scratches regions. The scale bars in A and B are 20 μm .

4. Conclusion

The nucleation and growth of Si nIs on c-Si substrates were observed. SEM and TEM measurements show that the formation of Si nIs can be controlled by the deposition parameters. The density and size of the nano islands can be reduced by either decreasing the excess Si concentration or incorporating N in the SRO. It has been shown that high density of epitaxial crystalline Si nIs can be produced on the Si substrate surface in an easy way, which is compatible with silicon technology. Substrate surface treatment can change the formation of Si nIs. A combination of structural and optical features is possible using a multi-layer approach. Samples with double layers show Si nano structures and a high photoluminescence.

5. Acknowledgments

We thank the National Natural Science Foundation of China (NSF under contract number 50172061), CONACyT, Mexico and the DFG (Deutsche Forschungs Gemeinschaft) for financial support. The technical help from Dr. Carlos Zuñiga, Pablo Alarcon, Ignacio Juarez, Netzahualcoyotl Carlos and Adrian Itzmoyotl is appreciated.

6. References

1. H. Grabert and M.H. Devoret, *Single Charge Tunneling* (Plenum, New York, 1992).
2. C.S. Lent and P.D. Tougaw, Lines of interacting quantum-dot cells: A binary wire, *J. Appl. Phys.* **74**(10), 6227-6223 (1993).
3. J.D. Joannopoulos, R.D. Meade and J.N. Winn, *Photonic Crystals* (Princeton University Press, Princeton, N.J, 1995).
4. K. Yano, T. Ishii, T. Haschimoto, T. Kobayashi, F. Murai and K. Seki, Room-temperature single-electron memory, *IEEE Trans. Electron Devices* **41**(9), 1628-1638 (1994).
5. L. Zhuang, L. Guo and S.Y Chou, Silicon single-electron quantum-dot transistor switch operating at room Temperature, *Appl. Phys. Lett.* **72**(10), 1205-1207 (1998).
6. K. Yoo, A.-P. Li, Zhenyu Zhang, H.H. Weitering, F. Flack, M.G. Lagally and J.F. Wendelken, Fabrication of Ge nanoclusters on Si with a buffer layer-assisted growth method, *Surface Science* **546**(2-3), L803-L807 (2003).
7. Kwonjae Yoo, Zhenyu Zhang and John F. Wendelken, A Novel Growth Approach of Ultrasmall Ge and Si Nanoclusters on a Si(100) Substrate without a Wetting Layer, *Jpn. J. Appl. Phys.* **42**(10B), L1232-L1234 (2003).
8. A. Olzierski, A. G. Nassiopoulou, I. Raptis and T. Stoica, Two-dimensional arrays of nanometre scale holes and nano-V-grooves in oxidized Si wafers for the selective growth of Ge dots or Ge/Si hetero-nanocrystals, *Nanotechnology* **15**(11), 1695-1700 (2003).
9. Qiming Li, Bellisppa Pattada, Steve R. J. Brueck, Stephen Hersee and Sang M. Han, Morphological evolution and strain relaxation of Ge islands grown on chemically oxidized Si(100) by molecular-beam epitaxy, *J. Appl. Phys.* **98**(7), 073504 (2004).
10. J. Tersoff, B J Spencer, A Rastelli and H. von Kanel, Barrierless Formation and Faceting of SiGe Islands on Si(001), *Phys. Rev. Lett.* **89**(19), 196104 (2002).
11. K. Matsumoto, M. Ishii, K. Sagawa, Y. Oka, B.J. Vartanian and J.S. Harris, Room temperature operation of a single electron transistor made by the scanning tunneling microscope nanooxidation process for the TiO_x/Ti system, *Appl. Phys. Lett.* **68**(1), 34-36 (1996).

12. P.A. Fontaine, E. Dubois and D. Stiévenard, Characterization of scanning tunneling microscopy and atomic force microscopy-based techniques for nanolithography on hydrogen-passivated silicon, *J. Appl. Phys.* **84**(4), 1776-1781 (1998).
13. F. Koch and V. Petrova-Koch, Light from Si-nanoparticle systems - a comprehensive view, *J. Non-Cryst. Solids* **198-200**(2), 840-846 (1996).
14. K. Kohon, Y. Osaka, F. Toyomura and H. Katayama, Photoluminescence of Si Microcrystals Embedded in SiO₂ Glass Films, *Jpn. J. Appl. Phys.* **33**(1),6616-6622 (1994).
15. Y. Kanzawa, T. Kageyama, S. Takeoka, M. Fujii, T. Hayashi and K. Yamamoto, Size-dependent near-infrared photoluminescence spectra of Si nanocrystals embedded in SiO₂ matrices, *Solid State Commun.* **102**, 533-537 (1997).
16. L. Patrone, D. Nelson, V.I. Safarov, M. Sentis, W. Marine and S. Glorico, Photoluminescence of silicon nanoclusters with reduced size dispersion produced by laser ablation, *J. Appl. Phys.* **87**(8), 3829-3837 (2000).
17. A.V. Sachenko, E.B. Kaganovich, E.G. Manoilov and S.V. Svechnikov, Kinetics of exiton photoluminescence in low-dimensional silicon structures, *Semiconductors* **35**(12), 1383-1389 (2001).
18. U. Kahler and H. Hofmeister, Silicon nanocrystallites in buried SiO_x layers via direct wafer bonding, *Appl. Phys. Lett.* **75**(5), 641-643 (1999).
19. H. Rinnert, M. Vergnat, G. Marchal and L.A. Burneau, Strong visible photoluminescence in amorphous SiO_x and SiO_x:H thin films prepared by thermal evaporation of SiO powder, *J. Lumin.* **80**(1-4), 445-448 (1999).
20. Z.Yu, M. Aceves, A. Luna, J.Du and D. Bian, Formation of silicon nanoislands on crystalline silicon substrates by thermal annealing of silicon rich oxide deposited by low pressure chemical vapour deposition, *Nanotechnology* **19**, 4962-4965 (2006).
21. Y. Shigeta, H. Fujino and K. Maki, Formation of uniform nanoscale Si islands on a Si(111)-7 × 7 substrate, *J. Appl. Phys.* **86**(2), 881-883 (1999).
22. R. Negishi, M. Suzuki and Y. Shigeta, Study of photoelectron spectroscopy from extremely uniform Si nanoislands on Si(111) 7×7 substrate, *J. Appl. Phys.* **96**(9), 5013-5016 (2004).
23. R. Nuryadi, Y. Ishikawa and M. Tabe, Formation and ordering of self-assembled Si islands by ultrahigh vacuum annealing of ultrathin bonded silicon-on-insulator structure, *Applied Surface Science* **159-160**, 121-126 (2000).
24. A.A. ShklyaeV and M. Ichikawa, Three-dimensional Si islands on Si(001) surfaces, *Phys. Rev. B* **65**(4), 045307 (2002).
25. A. Verevkin, A. Pearlman, W. Slysz, J. Zhang, M. Currier, A. Korneev, G. Chulkova, O. Okunev, P. Kouminov, K. Smirnov, B. Voronov, G. N. Gol'tsman, Roman Sobolewski, Ultrafast superconducting single-photon detectors for near-infraredwavelength quantum communications, *J. Modern Optics* **51**(9-10), 1447-1458 (2004).
26. M. Aceves, A. Malik and R. Murphy, *Sensors and Chemometrics* (Maria Teresa Ramirez-Silva et al (Eds.), Research Signpost, India, 2001).
27. B. H. Agustine, E. A. Irene, Y. J. He, K. J. Price, L. E. McNeil, K. N. Christensen and D. M. Maher, Visible light emission from thin films containing Si, O, N, and H, *J. Appl. Phys.* **78**(6), 4020-4030 (1995).
28. J.Y. Jeong, S. Im, M.S. Oh, H.B. Kim, K.H. Chae, C.N. Whang and J.H. Song, Defect versus nanocrystal luminescence emitted from room temperature and hot-implanted SiO₂ layers, *J. Lumin.* **80**(1-4), 285-289 (1999).
29. L. Khomenkova, N. Korsunskaya, M. Sheinkman, T. Stara, T.V. Torchynska and H.V. Hernandez, Radiative channel competition in silicon nanocrystallites, *J. Lumin.* **115**(3-4), 117-121 (2005).